J Mater Sci: Mater Med (2008) 19:3535–3544
DOI 10.1007/s10856-008-3531-1

# Blends of poly(3-hydroxybutyrate) and poly(p-dioxanone): miscibility, thermal stability and biocompatibility

**Michelle Dias · M. Cecilia Moraes Antunes · Arnaldo R. Santos Jr. · M. Isabel Felisberti**

Received: 14 April 2008 / Accepted: 27 June 2008 / Published online: 15 July 2008


**Abstract** The miscibility, the thermal degradation and biocompatibility of the blends of two biodegradable and bioreabsorbable polymers, brittle polyhydroxybutyric acid (PHB) and flexible poly (p-dioxanone) (PPD) are reported. The blends were prepared by casting from chloroform solutions and analyzed by differential scanning calorimetry, dynamic mechanical analysis, scanning electron microscopy and thermal gravimetric analysis. The blends are immiscible and present promising morphology of a dense phase and a microporous phase, one or the other being the matrix, depending on the composition. Despite the immiscibility, the thermal stability under an inert atmosphere is improved for both polymers. The results obtained from toxicity tests showed that PHB/PPD blends do not present indirect or direct cytotoxicity as a substrate for cellular growth.

## 1 Introduction

Biodegradable and biocompatible polyesters have received a great deal of attention due to their potential applications in the human body [1, 2], such as reabsorbable surgical sutures, biodegradable molded plastics [3] and tissue engineering [4, 5]. One of the most studied biocompatible polyesters is poly(3-hydroxybutyrate) (PHB) [6], a thermoplastic from the group of the poly(hydroxyalkanoates) (PHAs), produced by fermentation by a large variety of bacteria [2]. Since PHB is produced by bacterial fermentation it has perfect stereoregularity and high purity, which results in a high degree of crystallinity (almost 80%) [7]. Thus, PHB has limits for practical applications due to this brittleness, with a relatively low impact resistance [1]. The reasons for the brittleness of PHB are the low nucleation density during the crystallization, resulting in large spherulites that exhibit inter-spherulitic cracks. Since the glass transition temperature is close to room temperature, secondary crystallization of the amorphous phase occurs during storage at room temperature [8]. Furthermore, as the melting temperature of PHB is around 180°C, the processing temperature should be at least 190°C, where thermal degradation proceeds rapidly, the acceptable residence time in processing equipment is only a few minutes [9], resulting in a narrow processing window. PHB degradation occurs through random chain scission resulting in terminations of crotonic acid and vinyl groups [10].

In order to develop a bone substitution material the biocompatibility between PHB and osteoblast cultures has been studied. Linhart et al. have studied the growth of osteoblast culture in composites of amorphous carbonated apatite (ACP) and poly-(R)-3-hydroxybutyrate and found an excellent cell proliferation [4]. Despite the compatibility, a bone substitution material must be mechanically resistant. Wang et al. reported improvement in mechanical properties and osteoblast responses including cell growth in a composite of PHB and hydroxyapatite (HAP) [11]. Another possible way to improve mechanical properties is a blend with another biocompatible polymer with better mechanical properties. Depending on the miscibility of the two polymers, modification of physical characteristics such as glass transition temperature, crystallinity, density and

M. Dias · M. C. M. Antunes · M. I. Felisberti (✉)
Instituto de Química, Universidade Estadual de Campinas, CP 6154, 13083-970 Campinas, SP, Brazil
e-mail: misabel@iqm.unicamp.br

A. R. Santos Jr.
Departamento de Biologia Aplicada, Faculdade de Ciências Agrárias e Veterinárias, UNESP, Jaboticabal, SP, Brazil

morphology [12] can occur, resulting in a new material with new mechanical and thermal properties.

This paper presents a study of properties of blends of PHB and poly(p-dioxanone) (PPD), both biocompatible and biodegradable polyesters. Their chemical structures are presented in Fig. 1. PPD is a semicrystalline polymer produced by the polymerization of p-dioxanone in the presence of an organometallic catalyst [13, 14]. PPD degrades by hydrolytic processes at high degradation rates, generally resulting in low molar mass molecules that can be metabolized or bioreabsorbed by the body [15, 16]. The presence of an ether bond and an additional –CH2– in its structure result in a material with high flexibility and good mechanical properties [17], so that it is widely used in the medical field as biodegradable sutures.

Miscible blends have been prepared by mixing PHB with other polymers such as poly(vinyl acetate) [18], poly(vinylidene fluoride) [19] and cellulose acetate butyrate [20]. The copolymer poly(3-hydroxybutyrate-co-3-hydro xyhexanoate) is known to be miscible with 4,4-dihydro xydiphenylpropane [21] and with methoxy poly(ethylene glycol) [22]. The blends of PHB with poly(epichlorohydrin) and poly(epichlorohydrin-co-ethylene oxide) are known to be immiscible depending on the molar mass [23], as well as the blends with poly(cyclohexyl methacrylate) [24], poly(L-lactide) [25–27], poly(vinyl butyral) [28], poly(methylene oxide) [29], poly(butylene succinate)[30] and poly(caprolactone) [31]. However, studies of blends of PPD are rare. Pezzin et al. [32] studied blends of PPD and poly(L-lactic acid) (PLLA). Analyses suggested immiscibility between the polymers but some compositions showed improvement in mechanical properties [32]. This material was developed as a polymer scaffold to be used as temporary meniscal prosthesis to stimulate the formation of an in situ meniscal replication while the scaffold is reabsorbed by the organism [33].

In this work, blends of PHB/PPD with different compositions were prepared by casting. Differential scanning calorimetry (DSC) and dynamic mechanical analysis (DMA) were performed in order to study the miscibility. The blend morphology was studied using scanning electron microscopy (SEM). The influence of the PPD on the thermal degradation of PHB was investigated by thermogravimetrical analysis (TGA). The information obtained in this work could be useful to the development of a biomaterial suitable for tissue engineering.

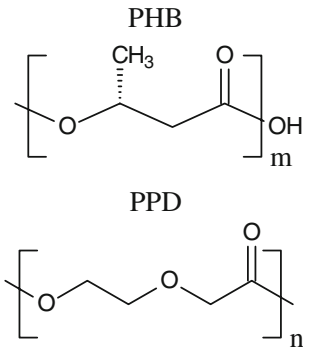


**Fig. 1** Chemical Structures of PHB and PPD

## 2 Experimental section

### 2.1 Materials

PHB (Mn 450000 g/mol$^{-1}$, melting point of ~180°C) was supplied by PHB do Brasil Ltda and PPD (melting point of ~100°C) was supplied by ETHICON INC. Both polymers were used as received.

### 2.2 Blend preparations

PHB was dissolved in dry chloroform under reflux. PPD was heated to 150°C and helded at this temperature for 10 min, then quenched in liquid nitrogen. This procedure was necessary because semicrystalline PPD solubilization in chloroform is very slow. The quenched PPD was dissolved in dry chloroform under reflux conditions. The polymer solutions were mixed resulting in the following compositions of PHB/PPD: 100/0, 80/20, 60/40, 50/50, 40/60, 20/80 and 0/100 (wt%/wt%). The mixtures were stirred for 24 h and then transferred to glass plates, which were maintained in a glass box for 24 h, under a controlled flow of argon, followed by drying under an inert atmosphere for 1 week. After that, the films were maintained under vacuum at 25°C for 24 h.

### 2.3 Blend characterization

DSC measurements were performed on a TA Instruments DSC2910 apparatus. Samples of 4–6 mg, sealed in aluminum pans, were first heated to 200°C, maintained at this temperature for 2 min, thus eliminating the thermal history, cooled to −40°C, maintained at this temperature for 2 min and finally heated to 200°C. Cooling and heating scans were performed at the rate of 10°C/min in an argon atmosphere. DSC curves were normalized with respect to the sample mass.

DMA analysis were conducted on a Rheometric Scientific DMTA V equipment in the tensile mode using films of blend samples with dimensions of 20.0 × 1.5 × 5.0 mm. Samples were submitted to cooling to −100°C and then heated to 200°C, with an amplitude of deformation of 0.01%, heating rate of 2°C/min and frequency of 1 Hz. For the DMA analysis with frequency variation, samples were submitted to

cooling to −60°C and heated to 60°C, with an amplitude of deformation of 0.01%, heating rate of 2°C/min and frequencies of 0.1, 1, 10 and 100 Hz, in the tensile mode.

For the electron microscopy (SEM) blends samples were immersed and kept in liquid nitrogen for a few minutes and then fractured in this state to induce a brittle fracture of the materials. After that, the samples were coated with Au. SEM images of the fracture surfaces were obtained using a JEOL-JSM 6340 LV scanning electron microscope (SEM)(Midletown,WI) operated at an acceleration rate of 20 kV.

Thermal degradation was investigated using a TA Instruments TGA 2050 at a heating rate of 10°C/min in argon atmosphere. Samples were cut into small circles with approximately the same diameter (3 mm) and heated from 30°C to 800°C.

## 3 Cytotoxicity test

### 3.1 Cell culture

Vero cells, a fibroblastic cell line established from the kidney of the African green monkey (*Cercopithecus aethiops*), were obtained from the Adolfo Lutz Institute, São Paulo, Brazil. Vero cells are recommended for studies of cytotoxicity and cell-substratum interactions in biomaterial research [34]. The cells were cultured at 37°C in Ham-F10 medium (Sigma Chemical Co., St. Louis, MO, USA) supplemented with 10% fetal calf serum (FCS, from Nutricell Nutrientes Celulares, Campinas, SP, Brazil).

### 3.2 Indirect toxicity test

This test was carried out according to ISO 10993-5. A solution of Ham F-10 medium with 10% of FCS and 10% of phenol was used as the positive control—a material that causes damaging effects on the cells. The negative control was a disposable polystyrene plate. Samples and controls were sterilized by keeping them for 48 h in pure ethanol.

The sterilized samples were placed in a 24-well polystyrene disposable plate, immersed in Ham-F10 medium with 10% FCS (in a proportion of 0.2 g per 1 ml of medium) and kept at 37°C for 24 h. After that, the culture medium was removed and a suspension of Vero Cells, in Ham-F10 with 10% FCS ($2 \times 10^5$ cell ml) was inoculated. The material was then incubated at 37°C for 24 h. The cells were observed in contrast phase using an Olympus IX-50 inverted microscope.

### 3.3 Direct toxicity test

To allow the assessment of Vero cells proliferation and morphology in direct contact with PHB/PPD blends, these fibroblasts were seeded directly over samples and controls in a Ham F-10 medium with 1% in weight for 24 h at 37°C. The cells were observed in contrast phase using an Olympus IX-50 inverted microscope.

In order to quantify the results of toxicity tests, there were counted 5 random fields from each well and established the mean and standard deviation. One way ANOVA at a significance level of $P \leq 0.05$ was used as statistical method in order to compare the controls and the samples.

## 4 Results and discussion

In order to study the miscibility of PHB/PPD blends DSC runs were performed. The cooling and second heating curves for the neat polymers and their blends are shown in Figs. 2 and 3. The data obtained from Figs. 2 and 3 are summarized in Table 1. A single exothermic peak, related to the crystallization process can be observed for the polymers and all blends (Fig. 2). PHB shows an intense crystallization peak with maximum at 57°C, while PPD shows a broader peak with maximum at 37°C. Blends containing 20, 40 and 80%wt of PPD show a main peak and a shoulder at temperatures close to the crystallization temperatures of the pure polymers. The crystallization peak of the blend with 60% of PPD is broader while for the blend with 80 wt% PPD the main peak is shifted to a higher temperature (maximum at 64°C) and the shoulder appears

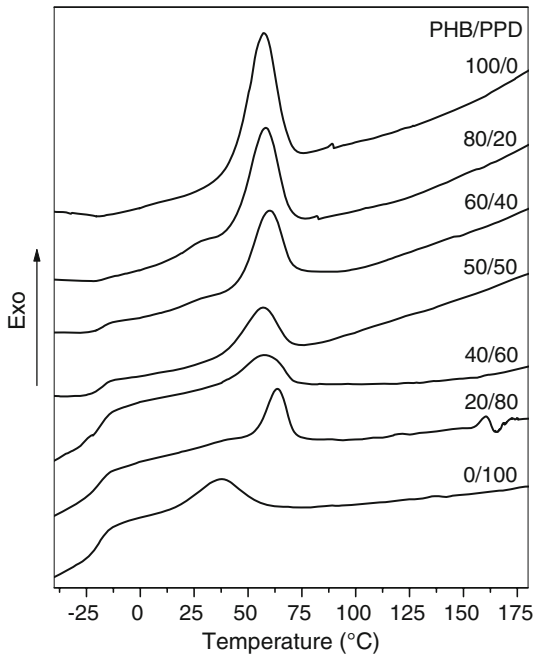


**Fig. 2** DSC curves of PHB/PPD blends with different composition of cooling process from melted state at the rate of 10°C/min and normalized with respect to the sample mass

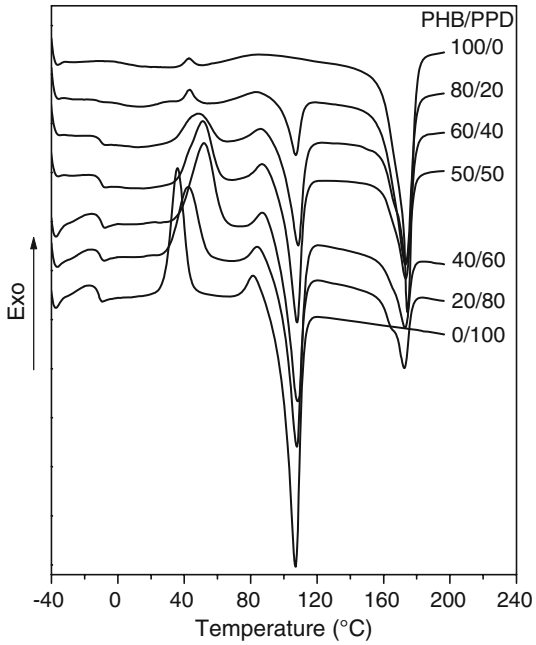


**Fig. 3** DSC curves of PHB/PPD blends with different composition of second heating at the rate of 10°C/min and normalized with respect to the sample mass

at 43°C. The cooling curves also show a glass transition around −10°C for all blend compositions (Fig. 2).

The second heating scan for neat PHB (Fig. 3) shows a small exothermic peak with maximum at 43°C attributed to cold crystallization and a broad exothermic peak in the temperature range from 50°C to 120°C, probably due to residual crystallization and reorganization. Above 160°C PHB melts and the endothermic peak presents a minimum at 173°C with a shoulder around 163°C. PPD presents a similar behavior. However, the cold crystallization at 36°C is more intense than for PHB. An exothermic peak close to melting is clear evidence of recrystallization. All blends present at least one exothermic peak, possibly an overlap of the crystallization process of both polymers, and two endothermic peaks related to melting. The peak profiles and the temperatures ranges are practically the same for all blends of each crystalline phase. The intensity of the peaks changes with the blend compositions, as expected. Crystallization enthalpies determined from cooling scans decrease with an increase in the amount of PPD in the blend. On the other hand, crystallization enthalpies determined from second heating scans increase as the PPD amount increases, which shows that PPD does not crystallize completely upon cooling, and the crystallization process is completed during the second heating, at temperatures lower than the melting temperatures. The melting behavior of the blends indicates that two crystalline phases are present in the blends. Moreover, no significant shift is observed for the melting peaks of both polymers, indicating that the blends are possibly immiscible.

The crystallinity degree (Xc %) of the polymers in the blends was obtained from the data of the experimental melting enthalpy (ΔHm) normalized with the fraction of each component and using the enthalpy of the polymer with 100 wt% crystallinity ($\Delta H^0$ PHB = 146 J/g [7] and $\Delta H^0$ PPD = 102 J/g [12]). The values obtained for the crystallinity degree are shown in Table 1. The crystallinity degree of PHB is 58% and that of PPD is 86%. In general, the crystallinity degree of PHB and of PPD does not change at concentrations up to 60 wt% of PHB. However, for blends richer in PPD, the crystallinity degree shows a complex dependence on the blend composition. For example, the crystallinity degree of PHB in the blend containing 20 wt% of this polymer is 90%, almost 60% higher than the value for pure PHB. On the other hand, the crystallinity degree of the PPD phase is lower for the blend PHB/PPD 20/80 and higher for the blends 40/60 and 50/50, compared to pure PPD. These results suggest an influence of one polymer on the kinetic crystallization process of the other. Similar results has been reported by Qiu et al. [35] for blends of poly(L-lactide) and poly(ethylene succinate).

The Fig. 4 shows DSC curves in the temperature range of the glass transition of both polymers. The DSC curves

**Table 1** Crystallization temperature ($T_c$) and enthalpy ($\Delta H_c$), melting temperature ($T_m$) and enthalpy ($\Delta H_m$), crystallinity degree ($X_c$) and glass transition for PHB/PPD blends with different compositions

| PHB/PPD | Cooling | | Second heating | | | | | | | | |
|---|---|---|---|---|---|---|---|---|---|---|---|
| | $T_c$ (°C) | $\Delta H_c$ (J/g) | $T_c$ (°C) | $\Delta H_c$ (J/g) | $T_m$ (°C) | | $\Delta H_m$ (J/g) | | $X_c$ (%) | | $T_g$ (°C) |
| | | | | | PHB | PPD | PHB | PPD | PHB | PPD | |
| 100/0 | 57 | 52 | 43 | 1 | 174 | – | 84 | – | 58 | – | – |
| 80/20 | 58 | 36 | 43 | 3 | 173 | 107 | 84 | 86 | 58 | 83 | – |
| 60/40 | 60 | 27 | 48 | 15 | 174 | 109 | 78 | 90 | 54 | 88 | −10 |
| 50/50 | 58 | 19 | 51 | 28 | 173 | 108 | 59 | 99 | 40 | 97 | −10 |
| 40/60 | 57 | 13 | 52 | 39 | 173 | 108 | 59 | 99 | 40 | 97 | −10 |
| 20/80 | 64 | 13 | 42 | 30 | 173 | 108 | 132 | 74 | 90 | 72 | −11 |
| 0/100 | 37 | 15 | 36 | 37 | – | 107 | – | 89 | – | 86 | −11 |

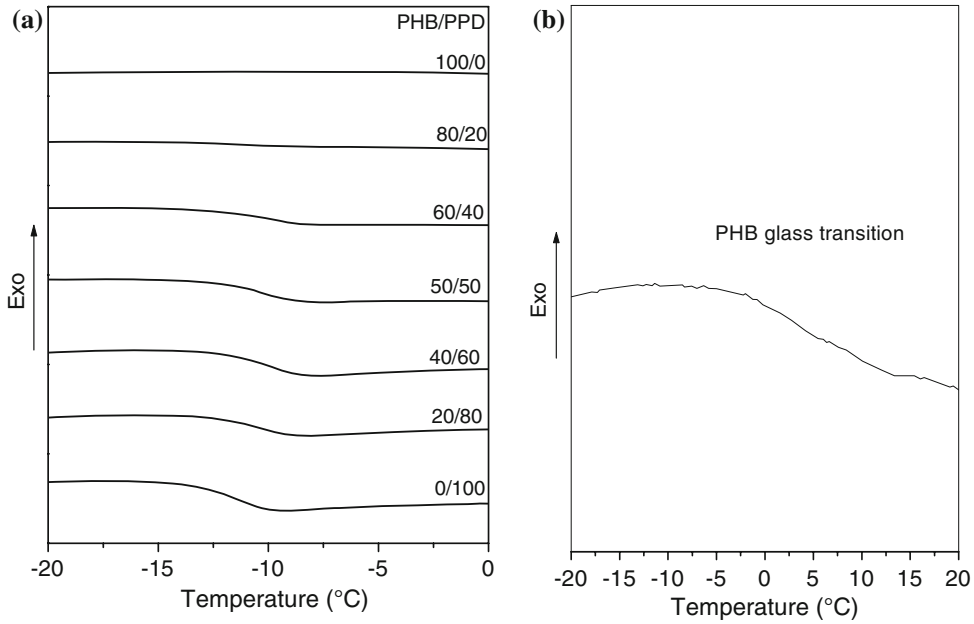


**Fig. 4** (**a**) DSC curves of PHB/PPD blends with different composition of second heating. (**b**) The glass transition region of PHB

shown in Fig. 4a are in the same scale and in this case the glass transition of PHB can not be observed. The glass transition of the PHB is shown in Fig. 4b. The $T_g$ for the polymers and their blends also shown in Table 1. The glass transition temperature ($T_g$) was taken as the temperature corresponding to the half width of the glass transition. Neat PPD shows a $T_g$ at −11°C, while the glass transition of neat PHB could not be observed in Fig. 4a because the high crystallinity degree. The $T_g$ for the blends is near the $T_g$ of PPD. As the percentage of PHB increases in the blend, the intensity of the glass transition decreases, making any discussion about miscibility based on the $T_g$ behavior impossible.

Apparently, only a single glass transition is observed for all blends, and in order to better investigate the phase behavior of this system, dynamic mechanical analysis, a sensitive technique to study polymer relaxation, was used. Figure 5 shows the loss modulus curves ($E'' \times T$) for the polymers and their blends in the temperature range of the glass transition of both polymers. The glass transition peak of neat PHB occurs between 0°C and 50°C, with a maximum at 25°C while neat PPD presents a glass transition peak between −25°C and 30°C with a maximum at 0°C. The curves of the blends show a broad peak between −25°C and 50°C on which shoulders at temperatures close to the maximum of the peaks for the pure polymers can be observed, except for the 50/50 PHB/PPD blend, that showed a single peak. The single peak could suggest miscibility but the glass transition for both polymers are very close, making difficult to conclude about the miscibility of PHB and PPD in the 50/50 blend. Thus, the DMA frequency assay was used in order to determine the activation energies associated with the glass transition. The

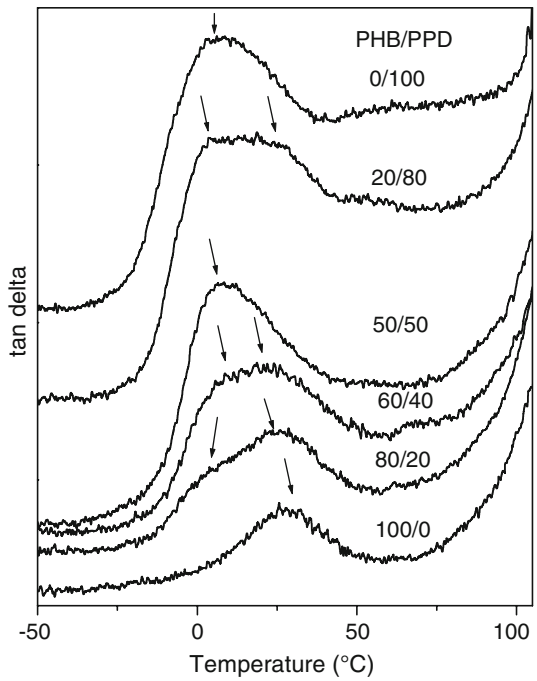


**Fig. 5** Data obtained from DMA analysis: tan $\delta$ at glass transition region of PHB/PPD blends

loss modulus curves for PHB, PPD and their blends at different frequencies are shown in Fig. 6.

The glass transition temperature was assumed to be the temperature corresponding to the maximum of the $E'' \times T$ peak. Some peaks also present a shoulder, however only the principal peak was considered in this analysis, because the determination of the maximum of the $E'' \times T$ peaks is more exact. The dependence of the $T_g$ on the frequency

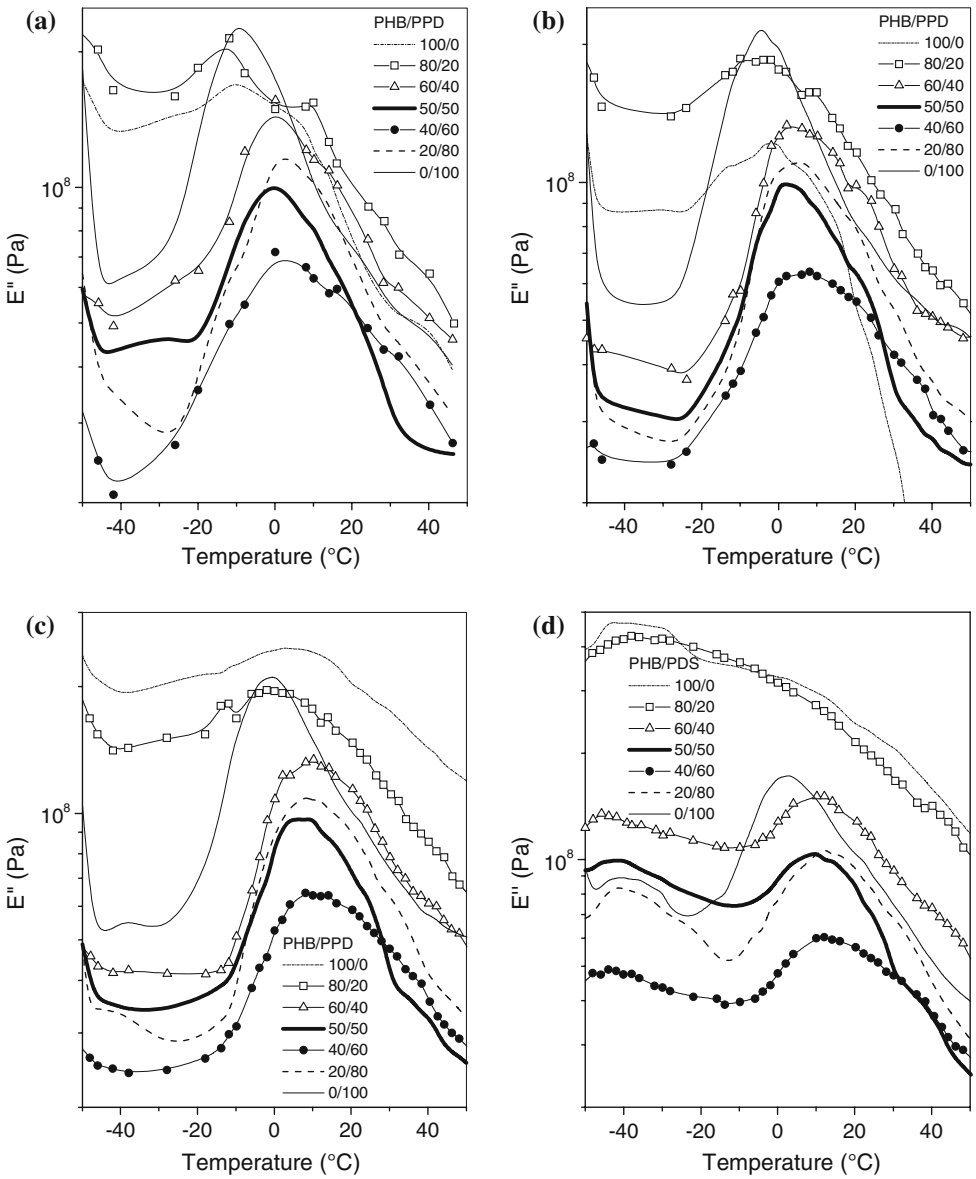


**Fig. 6** Loss modulus (E″) curves of PHB/PPD blends and neat polymers at different frequencies: 0.1 (**a**), 1 (**b**), 10 (**c**), and 100 Hz (**d**)

allow the determination of the activation energy of the glass transition using the Arrhenius equation:

$$k = A \cdot e^{-Ea/RT} \quad (1)$$

where *Ea* is the Arrhenius activation energy; *k*, the rate constant; *A*, the pre exponential factor; *R*, the general gas constant; and *T*, the temperature. The plot of the logarithm of the inverse of the frequency as a function of $1/T_g$ should give a straight line whose angular coefficient is *Ea*/*R*. The values of $T_g$ as a function of the frequency as well as the Ea for all the compositions are shown in Table 2.

The activation energy for the glass transition of PHB is $2.34 \times 10^5$ J mol$^{-1}$and for PPD is $3.51 \times 10^5$ J mol$^{-1}$. PHB crystallinity is lower than the crystallinity degree of PPD (Table 1) and this may explain the lower Ea for PHB glass transition. Except for the blend containing 80 wt% of PHB, the activation energy calculated for the main glass transition is similar to Ea for PPD, which indicates that the maximum used for calculations corresponds to the PPD glass transition peak. For the blend containing 80 wt% of PHB the Ea is close to the value of the pure PHB, indicating that the maximum used to calculate Ea corresponds to the glass transition of pure PHB. These results show that PHB/PPD blends present at least two phases, one of them constituted by one of the blend components. Therefore, the blends are immiscible throughout the whole composition range.

The Fig. 7 shows the storage modulus curves as a function of temperature ($E' \times T$) for neat PHB, PPD and their blends. The $E' \times T$ curve for neat PHB presents three drops: about 0°C, corresponding to the glass transition, about 120°C, related to secondary relaxation of the crystalline phase, and a

**Table 2** Glass transition temperature as a function of the frequency and the activation energy for the E″ × *T* peak associated with the glass transition

| PHB/PPD | $T_g$ (K) | | | | $E_a$ (kJ/mol) | Correlation factor |
|---|---|---|---|---|---|---|
| | 0.1 Hz | 1 Hz | 10 Hz | 100 Hz | | |
| 100/0 | 265 | 271 | 277 | – | 264 | 0.99992 |
| 80/20 | 262 | 269 | 275 | – | 211 | 0.99831 |
| 60/40 | 273 | 275 | 283 | 283 | 340 | 0.93352 |
| 50/50 | 273 | 275 | 281 | 283 | 392 | 0.97618 |
| 40/60 | 273 | 277 | 281 | 285 | 372 | 0.99992 |
| 20/80 | 273 | 279 | 281 | 285 | 376 | 0.97928 |
| 0/100 | 265 | 269 | 273 | 277 | 351 | 0.99991 |

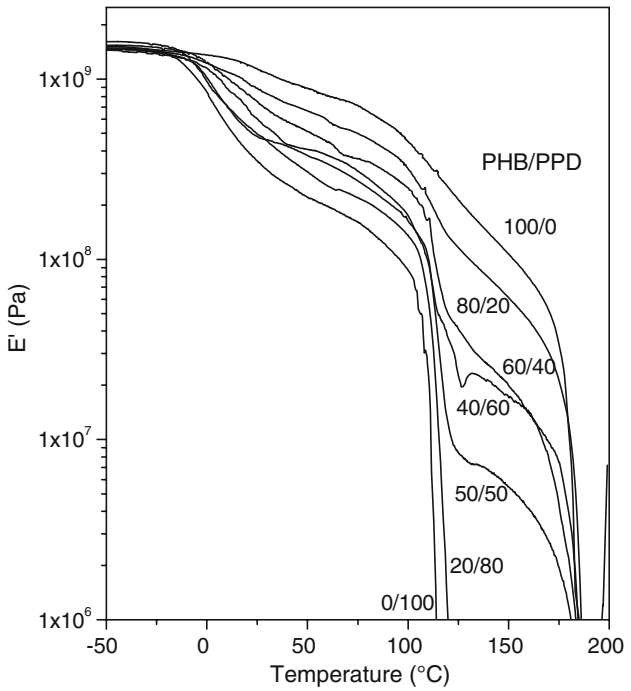


**Fig. 7** Storage modulus (E′) for PHB/PPD blends

third one at 170°C, related with the melting process. The storage curve for neat PPD presents two drops at about 0°C and 120°C, related to glass transition and melting, respectively. The E′ x *T* curves for the blends show three drops. The first is attributed to the overlap of the glass transition of both polymers, and the second and third drops are attributed to melting of PPD and PHB, respectively. Comparing the curves in the temperature range between the melting of PPD and PHB, it is evident that only the blend containing 80 wt% of PPD flows at the melting temperature of PPD. This means the matrix is PPD and PHB is the disperse phase. For the other blends, the storage modulus drops drastically only above the melting temperature of PHB, showing that the matrix is PHB.

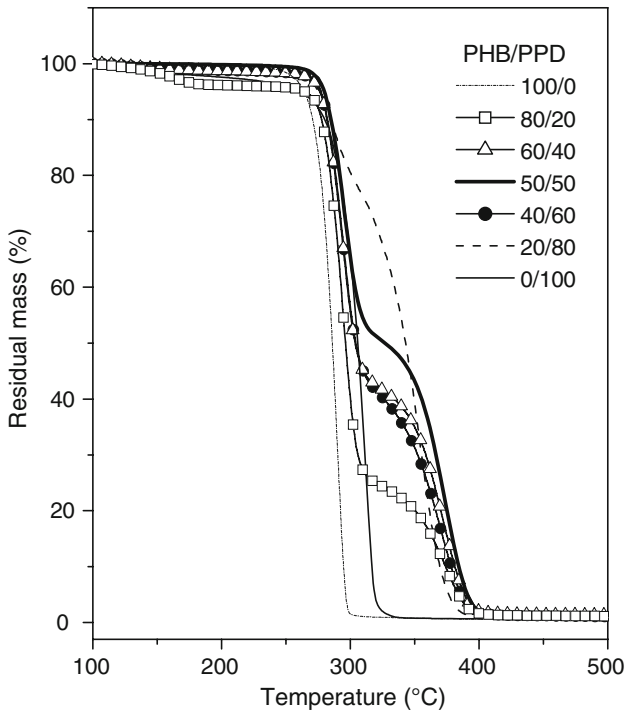


**Fig. 8** Thermogravimetric curves of PHB/PPD blends and neat polymers

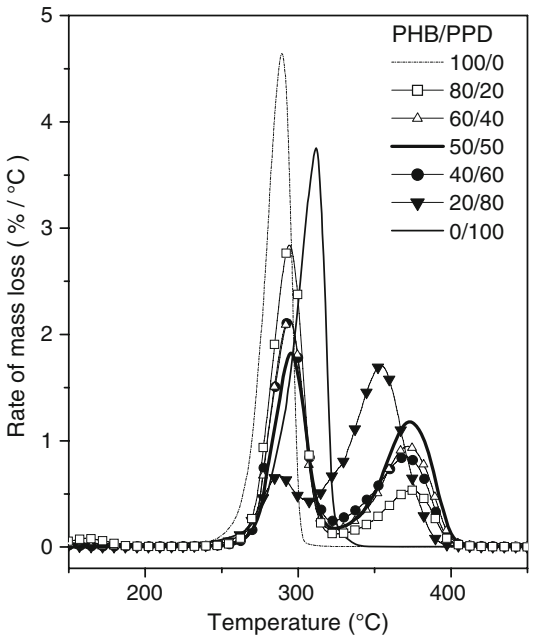


**Fig. 9** Derivative thermogravimetric curves of PHB/PPD blends and neat polymers

In order to study the thermal stability of the polymers and their blends, thermogravimetrical analyses were performed. Figure 8 shows the thermogravimetric curves (TG) and Fig. 9 the corresponding derivative thermogravimetric curves (DTG) for the PHB/PPD blends and neat polymers.

PHB and PPD degrade in a single-stage decomposition, which is represented by a single peak in the DTG curves. On the other hand, the blends have two-stage decompositions. The mass variation of each degradation step, determined from TGA curves (Fig. 8), was compared to the mass fraction of each polymer component in the blends. This analysis led to the conclusion that the first stage corresponds to the decomposition of PHB and the second stage to the decomposition of PPD. The temperature of the start of the degradation ($T_{onset}$) and the temperature corresponding to the maximum of the peak in the DTG curves, that is the temperature corresponding to the maximum rate of degradation ($T_{max}$), are summarized in Table 3.

**Table 3** $T_{onset}$ and $T_{max}$ for PHB and PPD for different compositions of PHB/PPD

| PHB/PPD | $T_{onset}$ (°C) | | $T_{max}$ (°C) | |
|---|---|---|---|---|
| | PHB | PPD | PHB | PPD |
| 100/0 | 273 | – | 289 | – |
| 80/20 | 280 | 353 | 294 | 374 |
| 60/40 | 279 | 351 | 294 | 371 |
| 50/50 | 279 | 352 | 295 | 373 |
| 40/60 | 281 | 349 | 294 | 371 |
| 20/80 | 270 | 334 | 288 | 354 |
| 0/100 | – | 293 | – | 312 |

PHB degradation starts at 273°C and PPD starts at 294°C. Table 3 shows that $T_{onset}$ of the PHB phase in the blends is slightly higher than the value for PHB. On the other hand, a significative shift to higher temperature is observed for the PPD phase in the blends, in comparison with pure PPD. Similar behavior is observed for $T_{max}$, which is higher for the blends in comparison with the neat polymers, except for the blend containing 20% of PHB. Thus, the degradation of one polymer appears to affect the mechanism of degradation of the other.

In order to better understand this stabilization process the kinetics of thermal decomposition of the blend containing 60% of PHB was studied. In this study, the Kissinger method [36] was used to determine the activation energy for the thermal decomposition and a value of 70 kJ/mol was found for pure PPD and 120 kJ/mol for PPD in the blend. This difference reinforces the hypothesis of the thermal stabilization of PPD in the presence of PHB.

The thermal stabilization is also reported for blends of PHB with dendrimers [37]. Since PHB is not stable at high temperatures, increases the thermal stability of the system is very important in order enable processing at higher temperatures.

The Fig. 10 presents SEM micrographs of the fracture surface of PHB/PPD blends. The micrographs show two distinct phases with a good interfacial adhesion, one porous and interconnected and the other one denser for all the

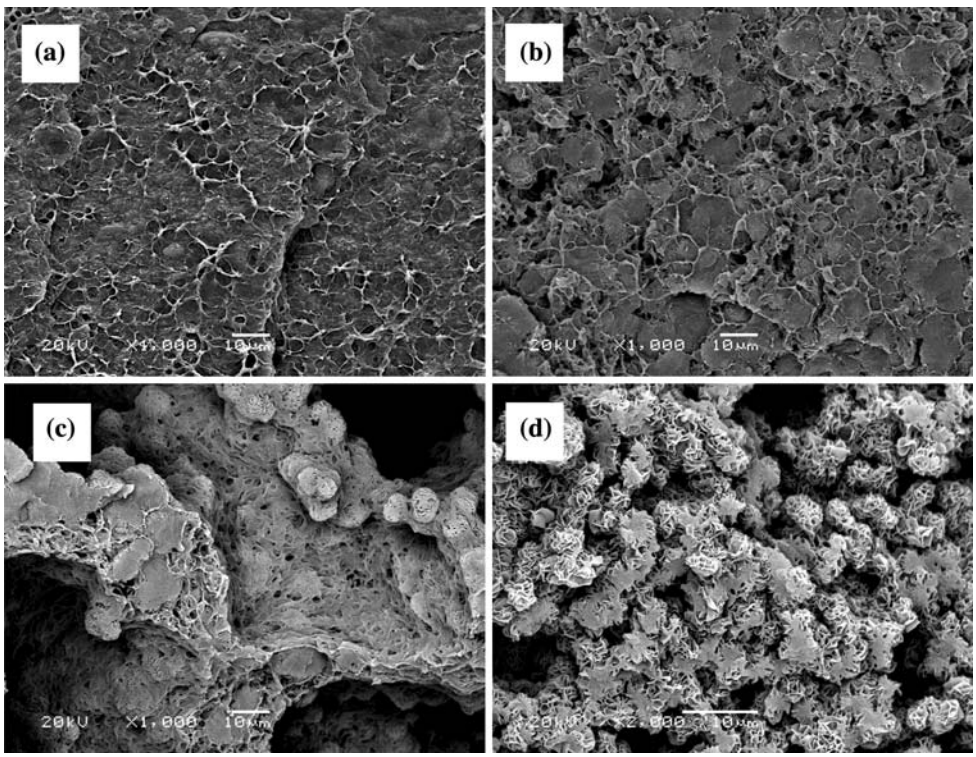


**Fig. 10** SEM Micrographs: (**a**) PHB/PPD: 20/80; (**b**) PHB/PPD: 40/60; (**c**) PHB/PPD: 60/40; (**d**) PHB/PPD: 80/20

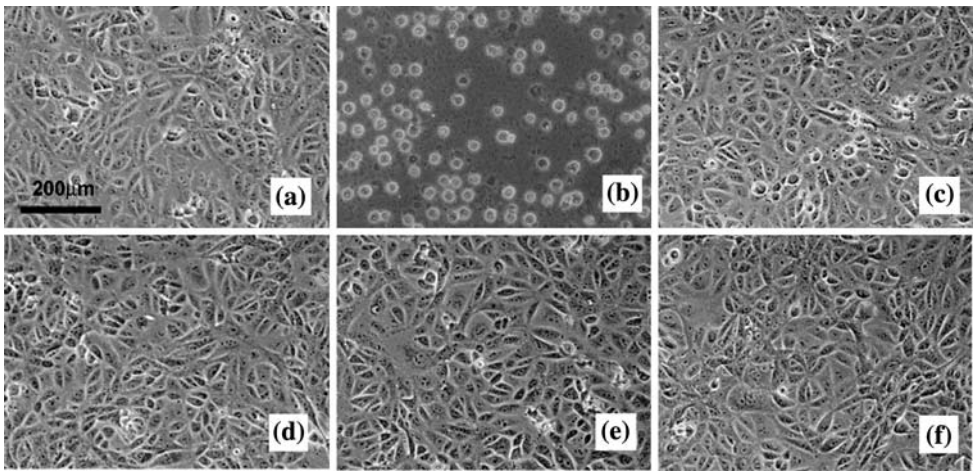


**Fig. 11** Indirect contact test of PHB, PPD and blends. (**a**) Negative control; (**b**) Positive Control; (**c**) PHB; (**d**) PHB/PPD 80/20; (**e**) PHB/PPD 20/80; (**f**) PPD

compositions, except for the blend containing 20 wt% of PHB. The morphology of the blend containing 20 wt% of PHB (matrix is PPD) is more uniform and with smaller pores. This porous structure makes PHB/PPD blend a promising system to be studied as biomaterial.

To be used as a biomaterial, a material should, besides assuming and keeping the necessary functions for the specific application, interact with the biological environment without causing any alterations in the organism. The initial step on biocompatibility is the evaluation of in vitro citotoxicity, which is based on morphological analysis and adhesion behavior [38–40].

The Fig. 11 presents the data referring to indirect cytotoxicity test. The Vero cells, which were grown in contact with a negative control, presented a flattened morphology, weak chromatin and evident nucleolus, indicating intense cell activity (Fig. 11a). The cells on the positive control surface (Fig. 11b) presented vacuolated morphology and cytoplasmatic fragmentation. The cells that were grown in contact with the neat polymers and its blends presented morphological patterns very similar to these of the negative control (Fig. 11c–g). The results of direct toxicity test are presented at Fig. 12, the same pattern observed in indirect toxicity test was observed in direct toxicity test.

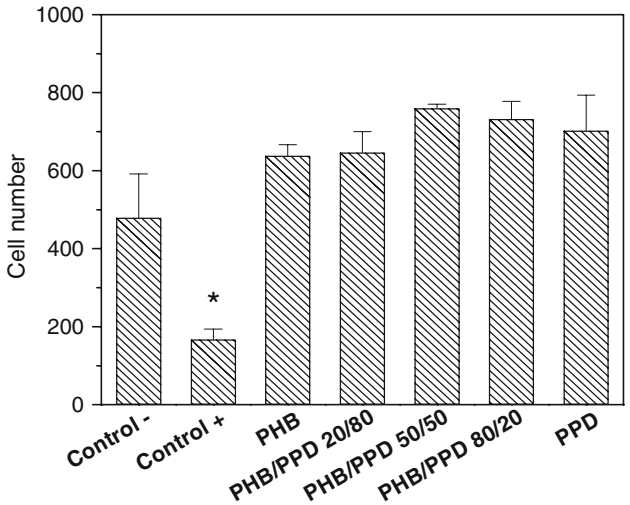


**Fig. 13** Indirect contact test: cell number of PHB, PPD, their blends, the positive and negative controls

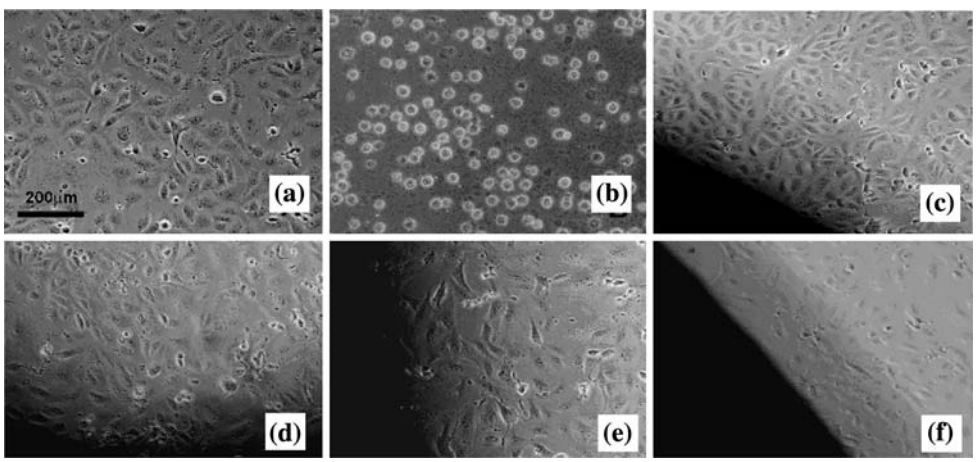


**Fig. 12** Direct contact test of PHB, PPD and blends. (**a**) Negative control; (**b**) Positive Control; (**c**) PHB; (**d**) PHB/PPD 80/20; (**e**) PHB/PPD 20/80; (**f**) PPD

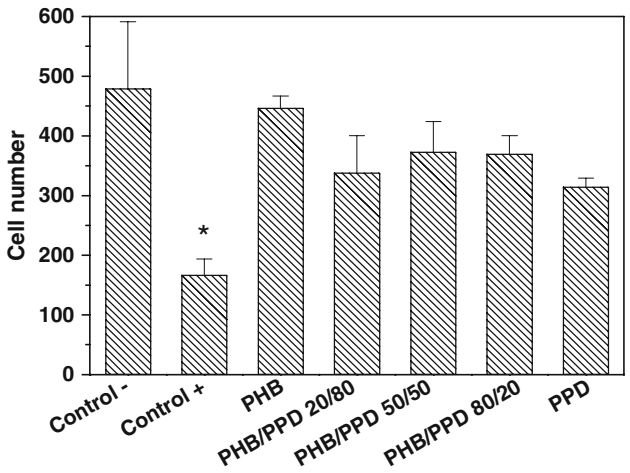


**Fig. 14** Direct contact test: cell number of PHB, PPD, their blends, the positive and negative controls

The cells quantification (Figs. 13 and 14) shows that the numbers of cells/well of the positive control is significantly lower than the other samples for both toxicity tests.

## 5 Conclusions

PHB and PPD blends are immiscible, however both crystallization kinetics and thermal degradation kinetics of these polymers are affected by the presence of one another. The blend morphologies are mostly porous and dependent on the composition. The results indicate that PHB/PPD blends do not present indirect or direct cytotoxicity as a substrate for cellular growth.

**Acknowledgement** We thank CNPq, FAPESP for financial support and the polymer suppliers: PHB do Brasil and Ethicon Inc.

## References

1. Z. Qiu, T. Ikehara, T. Nishi, Polymer (Guildf) **44**, 7519 (2003). doi:10.1016/j.polymer.2003.09.029
2. B.M.P. Ferreira, C.A.C. Zavaglia, E.A.R. Duek, J. Appl. Polym. Sci. **86**, 2898 (2002). doi:10.1002/app. 11334
3. E.E. Shafee, G.R. Saad, S.R. Fahmy, Eur. Polym. J. **37**, 1677 (2001). doi:10.1016/S0014-3057(01)00034-9
4. W. Linhart, W. Lehmann, M. Siedler, F. Peters, A.F. Schilling, K. Schwarz et al., J. Math. Sci. **41**, 4806 (2006). doi:10.1007/s10853-006-0023-x
5. P. Sangsanoh, S. Waleetorncheepsawat, O. Suwantong, P. Wutticharoenmongkol, O. Weeranantanapan, B. Chuenjitbuntaworn et al., Biomacromolecules **8**, 1587 (2007). doi:10.1021/bm061152a
6. R.W. Lenz, R.H. Marchessault, Biomacromolecules **6**, 1 (2005). doi:10.1021/bm049700c
7. L.M.W.K. Gunaratne, R.A. Shanks, G. Amarasinghe, Thermochim. Acta. **423**, 127 (2004). doi:10.1016/j.tca.2004.05.003
8. G.J.M. Koning, P.J. Lemstra, Polymer (Guildf) **34**, 4089 (1993). doi:10.1016/0032-3861(93)90671-V
9. M. Janigová, I. Lacík, I. Chodák, Polym. Degrad. Stab. **77**, 35 (2002). doi:10.1016/S0141-3910(02)00077-0
10. R. Lehrle, R. Willians, C. French, T. Hammond, Macromolecules **28**, 4408 (1995). doi:10.1021/ma00117a008
11. Y.-W. Wang, Q. Wu, J. Chen, G.-Q. Chen, Biomaterials **26**, 899 (2005). doi:10.1016/j.biomaterials.2004.03.035
12. S. Iannace, L. Ambrosio, S.J. Huang, L. Nicolais, J. Appl. Polym. Sci. **54**, 1525 (1994). doi:10.1002/app. 1994.070541017
13. H. Nishida, M. Yamashita, T. Endo, Y. Tokiwa, Macromolecules **33**, 6982 (2000). doi:10.1021/ma000457t
14. A.P.T. Pezzin, G.O.R. van Ekenstein, E.A.R. Duek, Polymer (Guildf) **42**, 8303 (2001). doi:10.1016/S0032-3861(01)00273-7
15. M.A. Sabino, J. Albuerne, A.J. Muller, J. Brisson, R.E. Prud'homme. Biomacromolecules **5**, 358 (2004). doi:10.1021/bm034367i
16. M.A. Sabino, G. Ronca, A.J. Muller, J. Math. Sci. **35**, 5071 (2000). doi:10.1023/A:1004831731756
17. M.A. Sabino, J.L. Feijoo, A.J. Muller, Polym. Degrad. Stab. **73**, 541 (2001). doi:10.1016/S0141-3910(01)00126-4
18. J.N. Hay, L. Sharma, Polymer (Guildf) **41**, 5749 (2000). doi:10.1016/S0032-3861(99)00807-1
19. J. Liu, Z. Qiu, B.-J. Jungnicke, J. Polym. Sci. Part B Polym. Phys. **43**, 287 (2005). doi:10.1002/polb.20274
20. G. Ceccorulli, M. Pizzoli, M. Scandola, Macromolecules **26**, 6722 (1993). doi:10.1021/ma00077a005
21. C. Chen, L. Dong, P.H.F. Yu, Eur. Polym. J. **42**, 2838 (2006). doi:10.1016/j.eurpolymj.2006.07.005
22. J.S. Lim, I. Noda, S.S. In, J. Polym. Sci. Part B Polym. Phys. **44**, 2852 (2006). doi:10.1002/polb.20937
23. J.A. Lima, M.I. Felisberti, Eur. Polym. J. **42**, 602 (2006). doi:10.1016/j.eurpolymj.2005.09.004
24. N. Lotti, M. Pizzoli, G. Ceccorulli, M. Scandola, Polymer (Guildf) **34**, 4935 (1993). doi:10.1016/0032-3861(93)90022-3
25. E. Blümm, A.J. Owem, Polymer (Guildf) **36**, 4077 (1995). doi:10.1016/0032-3861(95)90987-D
26. Y. Kikkawa, T. Suzuki, T. Tsuge, M. Kanesato, Y. Doi, H. Abe, Biomacromolecules **7**, 1921 (2006). doi:10.1021/bm0600163
27. T. Furukawa, H. Sato, R. Murakami, J.M. Zhang, Y.X. Duan, I. Noda et al., Macromolecules **38**, 6445 (2005). doi:10.1021/ma0504668
28. W. Chen, D.J. David, W.J. Macknight, F. Karaz, Polymer (Guildf) **42**, 8407 (2001). doi:10.1016/S0032-3861(01)00354-8
29. M. Avella, E. Martuscelli, G. Orsello, M. Raimo, B. Pascucci, Polymer (Guildf) **38**, 6135 (1997). doi:10.1016/S0032-3861(97)00166-3
30. Z. Qiu, T. Ikehara, T. Nishi, Polymer (Guildf) **44**, 2503 (2003). doi:10.1016/S0032-3861(03)00150-2
31. M.C.M. Antunes, M.I. Felisberti, Polímeros – Ciência e Tecnologia **15**, 134 (2005)
32. A.P.T. Pezzin, G.O.R.A. van Ekenstein, C.A.C. Zavaglia, G.T. ten Brinke, E.A.R. Duek, J. Appl. Polym. Sci. **88**, 2744 (2003). doi:10.1002/app. 11984
33. A.P.T. Pezzin, T.P. Cardoso, M.D.A. Rincon, C.A.C. Zavaglia, E.A.R. Duek, Artif. Organs **27**, 428 (2003). doi:10.1046/j.1525-1594.2003.07251.x
34. C.J. Kirkpatrick, Reg. Affairs **4**, 13 (1992)
35. J. Lu, Z. Qiu, W. Yang, Polymer (Guildf) **48**, 4196 (2007). doi:10.1016/j.polymer.2007.05.035
36. H.E. Kissinger, Anal. Chem. **29**, 1701 (1957). doi:10.1021/ac60131a045
37. S. Xu, R. Luo, L. Wu, K. Xu, J. Appl. Polym. Sci. **102**, 3782 (2006). doi:10.1002/app. 24742
38. C.M.A. Lopes, M.I. Felisberti, Biomaterials **24**, 1279 (2003). doi:10.1016/S0142-9612(02)00448-9
39. A.R. Santos, B.M.P. Ferreira, E.A.R. Duek, H. Dolder, R.S. Wada, M.L.F. Wada, Artif. Organs **28**, 381 (2004). doi:10.1111/j.1525-1594.2004.47199.x
40. A.R. Santos Jr., B.M.P. Ferreira, E.A.R. Duek, H. Dolder, M.L.F. Wada, Braz. J. Med. Biol. Res. **38**, 1623 (2005)